Published in final edited form as:
Science. 2011 November 11; 334(6057): 809–813. doi:10.1126/science.1209200.

Endocannabinoid hydrolysis generates brain prostaglandins that promote neuroinflammation**

Daniel K. Nomura[1,2,6,*], **Bradley E. Morrison**[3,6], **Jacqueline L. Blankman**[1], **Jonathan Z. Long**[1], **Steven G. Kinsey**[4], **Maria Cecilia G. Marcondes**[3], **Anna M. Ward**[1], **Aron H. Lichtman**[5], **Bruno Conti**[3], and **Benjamin F. Cravatt**[1,*]

[1]The Skaggs Institute for Chemical Biology and Department of Chemical Physiology, The Scripps Research Institute, 10550 N. Torrey Pines Road, La Jolla, CA 92037

[2]Program in Metabolic Biology, Department of Nutritional Sciences and Toxicology, University of California, Berkeley, 127 Morgan Hall, Berkeley, CA 94720

[3]Molecular and Integrative Neurosciences Department, The Scripps Research Institute, 10550 N. Torrey Pines Road, La Jolla, CA 92037

[4]Department of Psychology, West Virginia University, PO Box 6040, Morgantown, WV 26506

[5]Department of Pharmacology and Toxicology, Medical College of Virginia Campus, Virginia Commonwealth University, Richmond, VA 23298

Abstract

Phospholipase A2 (PLA2) enzymes are considered the primary source of arachidonic acid for cyclooxygenase (COX)-mediated biosynthesis of prostaglandins. Here, we show that a distinct pathway exists in brain, where monoacylglycerol lipase (MAGL) hydrolyzes the endocannabinoid 2-arachidonoylglycerol to generate a major arachidonate precursor pool for neuroinflammatory prostaglandins. MAGL-disrupted animals show neuroprotection in a parkinsonian mouse model. These animals are spared the hemorrhaging caused by COX inhibitors in the gut, where prostaglandins are instead regulated by cytosolic-PLA2. These findings identify MAGL as a distinct metabolic node that couples endocannabinoid to prostaglandin signaling networks in the nervous system and suggest that inhibition of this enzyme may be a new and potentially safer way to suppress the proinflammatory cascades that underlie neurodegenerative disorders.

Inflammation is a hallmark of many neurological disorders, including chronic pain, traumatic brain injury, neurodegenerative diseases, and stroke (1). Prominent among the known pro-inflammatory stimuli in the nervous system are prostaglandins, which are produced by cyclooxygenase enzymes (COX1 and COX2) (2) that are in neurons and glial cells (3). Rodents treated with COX inhibitors or lacking COX enzymes show protection in

*To whom correspondence should be addressed: dnomura@berkeley.edu and cravatt@scripps.edu.
[6]these authors contributed equally to this work

Author Contributions DKN, BFC wrote the paper; DKN, BEM, JLB, SGK, MCGM, AMW performed experiments; JZL provided reagents; DKN, BFC, BC, AH conceived and planned experiments.

Supporting Online Material
Materials and Methods
Figs. S1 to S11
Supplemental Table

models of neurodegenerative disorders that have an inflammatory component such as Parkinson's and Alzheimer's disease (4–6). However, the gastrointestinal and cardiovascular toxicities displayed by COX inhibitors have limited their translational potential for neuroinflammatory syndromes (7, 8 .

Phospholipase A2 (PLA2) enzymes, and cytosolic PLA2 (cPLA2 or *Pla2g4a*) in particular, have been viewed as the principal source of arachidonic acid (AA) for COX-mediated prostaglandin production (9); however, cPLA2-deficient mice have unaltered AA levels in brain (10). This finding, coupled with our recent observation that the genetic or pharmacological inactivation of monoacylglycerol lipase (MAGL, *Mgll*) in mice causes significant reductions in brain AA (11–13), led us to investigate the potential existence of non-PLA2 mechanisms that regulate prostaglandin production in the nervous system.

MAGL has been studied mostly for its role in hydrolyzing the endocannabinoid 2-arachidonoylglycerol (2-AG) (11, 14, 15). Consistent with previous investigations, we found that mice deficient in the gene that encodes MAGL *($Mgll^{-/-}$* mice) or mice treated with the MAGL-selective inhibitor JZL184 (40 mg/kg, i.p.) showed loss of MAGL activity (11, 12), but not other brain serine hydrolase activities (fig. S1A-B), and possessed elevated brain levels of 2-AG and corresponding reductions in AA (Fig. 1, A to C) (16). We more broadly profiled the metabolomic effects of MAGL disruption, using a combination of targeted and untargeted metabolomic approaches, and discovered by targeted analysis that inactivation of this enzyme also caused significant reductions in several prostaglandins and other eicosanoids in brain, including prostaglandin E2 (PGE2), PGD2, PGF2, and thromboxane B2 (TXB2) (Fig. 1, A to C, fig. S2A) (17). In contrast, other arachidonoyl-containing phospho- and neutral lipid species, including the second major endocannabinoid anandamide (AEA), as well as other free fatty acids were unaltered in brain tissue from MAGL-deficient animals (Fig. 1, A to C and fig. S3). These results indicate that the principal metabolic effects of disrupting MAGL in the brain are elevations in substrate MAGs, including 2-AG, and reductions in the product AA and downstream AA-derived eicosanoids.

We next asked whether MAGL also controls eicosanoid production in states of neuroinflammation. Mice were systemically administered the pro-inflammatory agent lipopolysaccharide (LPS) (18) (20 mg/kg ip) for two-six hr, after which animals were sacrificed and their brain lipids measured. LPS treatment produced a robust, time-dependent increase in brain eicosanoids (Fig. 1, B and C, fig. S2A and C), and these changes were markedly blunted in mice treated with JZL184 (Fig. 1B, fig. S2A) or in $Mgll^{-/-}$ mice (Fig. 1C, fig. S2A). Eicosanoids did rise significantly in brains from LPS-treated mice lacking MAGL; however, their levels did not substantially exceed the basal levels observed in untreated wild-type mice (Fig. 1, B and C, fig. S2A, fig. S4A). The impairment in brain eicosanoid production in MAGL-deficient animals was not reversed by cannabinoid receptor type 1 (CB1, *CNR1*) or type 2 (CB2, *CNR2*) antagonists rimonabant and AM630, respectively (1 mg/kg, ip, administered 30 min prior to JZL184) or in *Cnr1/Cnr2* $^{-/-}$ mice (fig. S4B), strengthening our conclusion that this metabolic effect is a direct consequence of reductions in AA rather than an indirect consequence of enhanced endocannabinoid signaling. COX1-selective (by SC560), but not COX2-selective (by celecoxib) inhibition, reduced both basal and LPS-induced brain eicosanoid levels, mirroring the metabolic effects caused by MAGL inactivation (fig. S4C). We also noted that LPS treatment did not alter brain AA levels, despite causing elevations in prostaglandins. This finding could be explained in the context of previous reports showing that LPS induces COX1 expression in the brain (19). A model thus emerges where LPS-induced COX1 shunts a small proportion of the high bulk levels of AA (20–100 nmol/g brain weight) towards PGs, which are found at much lower levels in brain (1–100 pmol/g brain weight). By controlling the quantity of

AA available to LPS-induced COX1, MAGL exerts a crucial control over brain PG production in both basal and neuroinflammatory states.

LPS treatment induces widespread elevations in pro-inflammatory cytokines, including interleukin (IL)1α, IL1β, IL6, and tumor necrosis factor (TNF)α (20). We found that pharmacological or genetic inactivation of MAGL, while not affecting basal cytokine levels, produced a near-complete blockade of LPS-induced elevations in brain cytokines (Fig. 2A, fig. S5A). This suppression of cytokines was not reversed by CB1 or CB2 antagonists or in *Cnr1/Cnr2*$^{-/-}$ mice (Fig. 2A, fig. S5B). Disruption of MAGL also blocked LPS-induced microglial activation (Fig. 2B, fig. S5C and D). SC-560 also reduced LPS-stimulated cytokine production in the brain, whereas celecoxib paradoxically further increased IL1α and IL1β levels in LPS-treated animals (fig. S6). These results are consistent with recent studies showing that mice deficient in COX1 and COX2 display attenuated and exacerbated neuroinflammatory responses to LPS-treatment, respectively (2, 20, 21).

Because previous studies have provided evidence that cPLA2 also plays a role in prostaglandin production and neuroinflammation (10, 22–24), we sought to assess the relative contributions of MAGL and cPLA2 to brain prostaglandin generation. Consistent with past reports (10, 22), we found that the basal levels of AA and prostaglandins, as well as general serine hydrolase activities, including MAGL, were unaltered in brain tissue from mice deficient in cPLA2 (*Pla2g4a*$^{-/-}$ mice) (25) (Fig. 3A and fig. S7A and B). A modest, but significant reduction (~20%) in LPS-induced prostaglandins was, however, detected in brains from *Pla2g4a*$^{-/-}$ mice (Fig. 3A), as has been reported previously (10, 22). This reduction was much lower in magnitude than the > 3-fold decrease in brain prostaglandins observed in MAGL-deficient animals. Interestingly, the effects of MAGL and cPLA2 blockade were additive: treatment with JZL184 produced greater reductions in brain prostaglandins in LPS-treated *Pla2g4a*$^{-/-}$ mice compared to LPS-treated *Pla2g4a*$^{+/+}$ mice (Fig. 3A). These data indicate that both MAGL and cPLA2 contribute to the AA pools for neuroinflammatory prostaglandins such that the combined inactivation of these enzymes completely blocks brain prostaglandin increases caused by LPS.

Intrigued by the different roles played by MAGL and cPLA2 in the brain, we expanded our analysis of these enzymes' contributions to prostaglandin metabolism to peripheral tissues. A clear partitioning of function was uncovered, with MAGL exerting control over both basal and LPS-induced AA and prostaglandins in liver and lung (Fig. 3, B and C), whereas cPLA2 regulated these lipids in gut and spleen (Fig. 3, D and E). We also found that elevations in pro-inflammatory cytokines were significantly blunted in lung and liver tissue from LPS-treated *Mgll*$^{-/-}$mice (fig. S8A and B). Neither MAGL nor cPLA2 made a substantial contribution to prostaglandin production in heart or kidney (fig. S8C and D), where distinct PLA2s (26) may regulate eicosanoid metabolic pathways. These findings reveal a clear anatomical segregation for the enzymatic pathways that supply the AA precursor of proinflammatory prostaglandins and further suggest that MAGL inactivation may avoid some of the major adverse pharmacological effects of COX inhibitors (7). Prominent among the toxicities caused by COX inhibitors is gastrointestinal bleeding (7). Consistent with our finding, JZL184 does not cause the gastric hemorrhaging that is observed with COX1 or dual COX inhibitors (fig. S9). On the contrary, recent data suggest that inhibition of MAGL by JZL184 exerts a CB1 receptor-dependent protective effect on COX inhibitor-induced gastric bleeding (27).

Many neurodegenerative disorders involve a strong inflammatory component (1). We tested the effects of MAGL blockade in the 1-methyl-4-phenyl-tetrahydropyridine (MPTP) mouse model of Parkinsonism, as COX inhibitors are known to be neuroprotective (4). Indeed, neuroprotection could be in part due to blocking PGE2 production, which is toxic to

dopaminergic neurons (28). We found that either pharmacologic (JZL184, 40 mg/kg, oral treatment once per day starting 24 h prior to MPTP treatment) or genetic inactivation of MAGL prevented MPTP-induced dopaminergic neuronal loss in the substantia nigra (Fig. 4, A and B, fig. S10A and B) and significantly attenuated dopaminergic neuronal terminal loss (fig. S10C) and dopamine reductions in both the substantia nigra and striatum (Fig. 4C, fig. S10D). These neuroprotective effects were accompanied by a blockade of MPTP-induced increases in brain AA, prostaglandins (Fig. 4D and fig. S10E), and pro-inflammatory cytokines (fig. S10F). MPTP treatment also led to elevations in brain 2-AG, which is a likely source for the MAGL-dependent increases in AA and prostaglandins (fig. S10G). Although cannabinoid agonists have previously been shown to protect against neurodegeneration in the MPTP model (29), the effects of MAGL blockade were not reversed by cannabinoid receptor antagonists (Fig. 4, A to C, fig. S10H), and were recapitulated by COX inhibition (fig. S10). Pharmacological or genetic disruption of MAGL did not affect the metabolism of MPTP to MPP+ (fig. S11). We conclude that the neuroprotective effects of MAGL inactivation are primarily due to reductions in AA and proinflammatory prostaglandins rather than augmentation of endocannabinoid signaling.

Mammals possess multiple COX enzymes (COX1 and COX2 (3)) that produce prostaglandins, and the functional characterization and selective targeting of these enzymes have led to drugs for treating pain disorders (2, 3). Here, we have discovered that a similar diversification exists for the enzymatic sources of AA coupled to prostaglandin production, which extend beyond PLA2 cleavage of phospholipids to include MAGL hydrolysis of the endocannabinoid 2-AG. This upstream branch point demarcates the anatomy of prostaglandin signaling in vivo, with MAGL exerting principal control over the tone and overall abundance of AA and prostaglandins in the brain and select peripheral tissues under both basal and inflammatory states. This discovery has translational implications in that we, and others, have found that neuroinflammatory prostaglandins derive in large part from COX1 (2, 20), which also produces these signaling lipids in the gut to protect against gastrointestinal damage (8). That cPLA2, rather than MAGL, provides the AA for prostaglandin biosynthesis in the gut suggests that MAGL inhibitors should avoid the gastrointestinal toxicity observed with COX1 inhibitors, a premise supported by our data (fig. S9). MAGL inhibitors, on the other hand, have been shown to downregulate CB1 receptors in specific brain regions and cause mild physical dependence following chronic treatment at high-doses (12), and these adaptations will need to be considered when judging the translational potential of MAGL as a target for neuroinflammatory and neurodegenerative disorders.

Supplementary Material

Refer to Web version on PubMed Central for supplementary material.

Acknowledgments

We thank the members of the Cravatt laboratory for helpful discussion and critical reading of the manuscript. We also thank Yun Kyung Hahnat Virginia Commonwealth University for experimental assistance. This work was supported by the National Institutes of Health (DA017259 (BFC), K99DA030908, R00DA030908 (DKN), 5P01DA009789 and P01DA017259 (AHL), AG028040 (BC, BEM), R03DA027936 (MCGM), DA026261 (JLB), T32DA007027 (SGK)), Institute for Drug and Alcohol Studies at Virginia Commonwealth University, the Ellison Medical Foundation, and the Skaggs Institute for Chemical Biology. A patent has been filed (US Patent Application Serial No. 12/998,642) “Methods and compositions related to targeting monoacylglycerol lipase” which relates to inhibitors of monoacylglycerol lipase and associated methods, compositions, and potential uses for treating human disorders that are associated with endocannabinoid signaling. Authors who are listed inventors are J.Z.L., D.K.N, B.F.C. The data reported in this paper are tabulated in the main text and supporting online material.

References

1. Glass CK, Saijo K, Winner B, Marchetto MC, Gage FH. Mechanisms underlying inflammation in neurodegeneration. Cell. Mar 19.2010 140:918. [PubMed: 20303880]
2. Rouzer CA, Marnett LJ. Cyclooxygenases: structural and functional insights. J Lipid Res. Apr.2009 50(Suppl):S29. [PubMed: 18952571]
3. Simmons DL, Botting RM, Hla T. Cyclooxygenase isozymes: The biology of prostaglandin synthesis and inhibition. Pharmacol Rev. Sep.2004 56:387. [PubMed: 15317910]
4. Teismann P, et al. Cyclooxygenase-2 is instrumental in Parkinson's disease neurodegeneration. Proceedings of the National Academy of Sciences of the United States of America. Apr 29.2003 100:5473. [PubMed: 12702778]
5. Choi SH, Bosetti F. Cyclooxygenase-1 null mice show reduced neuroinflammation in response to beta-amyloid. Aging-Us. Feb.2009 1:234.
6. McKee AC, et al. Ibuprofen reduces Abeta, hyperphosphorylated tau and memory deficits in Alzheimer mice. Brain Res. May 1.2008 1207:225. [PubMed: 18374906]
7. Ng SC, Chan FKL. NSAID-induced gastrointestinal and cardiovascular injury. Curr Opin Gastroen. Nov.2010 26:611.
8. Grosser T, Fries S, FitzGerald GA. Biological basis for the cardiovascular consequences of COX-2 inhibition: therapeutic challenges and opportunities. J Clin Invest. Jan.2006 116:4. [PubMed: 16395396]
9. Buczynski MW, Dumlao DS, Dennis EA. Thematic Review Series: Proteomics. An integrated omics analysis of eicosanoid biology. J Lipid Res. Jun.2009 50:1015. [PubMed: 19244215]
10. Rosenberger TA, Villacreses NE, Contreras MA, Bonventre JV, Rapoport SI. Brain lipid metabolism in the cPLA2 knockout mouse. J Lipid Res. Jan.2003 44:109. [PubMed: 12518029]
11. Long JZ, et al. Selective blockade of 2-arachidonoylglycerol hydrolysis produces cannabinoid behavioral effects. Nature chemical biology. Jan.2009 5:37.
12. Schlosburg JE, et al. Chronic monoacylglycerol lipase blockade causes functional antagonism of the endocannabinoid system. Nature neuroscience. Sep.2010 13:1113.
13. Nomura DK, et al. Activation of the endocannabinoid system by organophosphorus nerve agents. Nat Chem Biol. Jun.2008 4:373. [PubMed: 18438404]
14. Dinh TP, et al. Brain monoglyceride lipase participating in endocannabinoid inactivation. Proc Natl Acad Sci U S A. Aug 6.2002 99:10819. [PubMed: 12136125]
15. Lambert DM, Fowler CJ. The endocannabinoid system: drug targets, lead compounds, and potential therapeutic applications. J Med Chem. Aug 11.2005 48:5059. [PubMed: 16078824]
16. Materials and methods are available as supporting material on Science Online.
17. We found that MAGL similarly regulates brain AA and PG levels in mice sacrificed by decapitation (Fig. 1) or head-focused microwave irradiation (fig. S2), although the absolute levels of AA and eicosanoids were 5–20-fold lower in microwaved brains (fig. S2B). Microwaving has been introduced as a method of animal sacrifice to minimize post-mortem accumulation of AA and PG lipids in brain tissue (33, 34). Our data might therefore suggest that MAGL regulates both basal and ischemic pools of brain eicosanoids; however, we also evaluated brains that were removed from mice following decapitation and left to sit at room temperature for 20 min prior to processing, and found that MAGL did not regulate the dramatic increases in AA and PGs that were observed in these brain samples (fig. S2). These data thus indicate that MAGL does not control the major ischemia-induced pools of arachidonic acid and prostaglandins that are known to accumulate in post-mortem brain tissue (33, 34). Unless otherwise noted the remaining studies reported herein were performed with mice sacrificed by decapitation, which permitted parallel analysis of lipid levels and other biochemical parameters (e.g., enzyme activities, cytokine levels) that might otherwise be perturbed by brain microwaving.
18. Takeuchi O, Akira S. Pattern recognition receptors and inflammation. Cell. Mar 19.2010 140:805. [PubMed: 20303872]
19. Garcia-Bueno B, Serrats J, Sawchenko PE. Cerebrovascular cyclooxygenase-1 expression, regulation, and role in hypothalamic-pituitary-adrenal axis activation by inflammatory stimuli. The

Journal of neuroscience : the official journal of the Society for Neuroscience. Oct 14.2009 29:12970. [PubMed: 19828811]

20. Choi SH, Langenbach R, Bosetti F. Genetic deletion or pharmacological inhibition of cyclooxygenase-1 attenuate lipopolysaccharide-induced inflammatory response and brain injury. FASEB J. May.2008 22:1491. [PubMed: 18162486]
21. Aid S, Langenbach R, Bosetti F. Neuroinflammatory response to lipopolysaccharide is exacerbated in mice genetically deficient in cyclooxygenase-2. J Neuroinflammation. 2008; 5:17. [PubMed: 18489773]
22. Sapirstein A, et al. Cytosolic phospholipase A2alpha regulates induction of brain cyclooxygenase-2 in a mouse model of inflammation. Am J Physiol Regul Integr Comp Physiol. Jun.2005 288:R1774. [PubMed: 15718387]
23. Bonventre JV, et al. Reduced fertility and postischaemic brain injury in mice deficient in cytosolic phospholipase A2. Nature. Dec 11.1997 390:622. [PubMed: 9403693]
24. Sanchez-Mejia RO, et al. Phospholipase A2 reduction ameliorates cognitive deficits in a mouse model of Alzheimer's disease. Nat Neurosci. Nov.2008 11:1311. [PubMed: 18931664]
25. Bonventre JV, et al. Reduced fertility and postischaemic brain injury in mice deficient in cytosolic phospholipase A(2). Nature. Dec 11.1997 390:622. [PubMed: 9403693]
26. Lambeau G, Gelb MH. Biochemistry and physiology of mammalian secreted phospholipases A2. Annu Rev Biochem. 2008; 77:495. [PubMed: 18405237]
27. Kinsey SG, et al. Inhibition of monoacylglycerol lipase (MAGL) attenuates NSAID-induced gastric hemorrhages in mice. The Journal of pharmacology and experimental therapeutics. Jun 9.2011
28. Carrasco E, Casper D, Werner P. PGE(2) receptor EP1 renders dopaminergic neurons selectively vulnerable to low-level oxidative stress and direct PGE(2) neurotoxicity. Journal of neuroscience research. Nov 1.2007 85:3109. [PubMed: 17868147]
29. Price DA, et al. WIN55,212-2, a cannabinoid receptor agonist, protects against nigrostriatal cell loss in the 1-methyl-4-phenyl-1,2,3,6-tetrahydropyridine mouse model of Parkinson's disease. Eur J Neurosci. Jun.2009 29:2177. [PubMed: 19490092]
30. Smith CA, Want EJ, O'Maille G, Abagyan R, Siuzdak G. XCMS: processing mass spectrometry data for metabolite profiling using nonlinear peak alignment, matching, and identification. Anal Chem. Feb 1.2006 78:779. [PubMed: 16448051]
31. Raetz CR, et al. Kdo2-Lipid A of Escherichia coli, a defined endotoxin that activates macrophages via TLR-4. Journal of lipid research. May.2006 47:1097. [PubMed: 16479018]
32. Deems R, Buczynski MW, Bowers-Gentry R, Harkewicz R, Dennis EA. Detection and quantitation of eicosanoids via high performance liquid chromatography-electrospray ionization-mass spectrometry. Methods in enzymology. 2007; 432:59. [PubMed: 17954213]
33. Golovko MY, Murphy EJ. An improved LC-MS/MS procedure for brain prostanoid analysis using brain fixation with head-focused microwave irradiation and liquid-liquid extraction. Journal of lipid research. Apr.2008 49:893. [PubMed: 18187404]
34. Farias SE, Basselin M, Chang L, Heidenreich KA, Rapoport SI, Murphy RC. Formation of eicosanoids, E_2/D_2 isoprostanes, and docosanoids following decapitation- induced ischemia, measured in high-energy-microwaved rat. Journal of lipid research. May.2008 49:1990. [PubMed: 18503030]
35. Baquet ZC, Williams D, Brody J, Smeyne RJ. A comparison of model-based (2D) and design-based (3D) stereological methods for estimating cell number in the substantia nigra pars compacta (SNpc) of the C57BL/6J mouse. Neuroscience. Jul 21.2009 161:1082. [PubMed: 19376196]
36. Blankman JL, Simon GM, Cravatt BF. A comprehensive profile of brain enzymes that hydrolyze the endocannabinoid 2-arachidonoylglycerol. Chem Biol. Dec.2007 14:1347. [PubMed: 18096503]
37. Patricelli MP, Giang DK, Stamp LM, Burbaum JJ. Direct visualization of serine hydrolase activities in complex proteomes using fluorescent active site-directed probes. Proteomics. Sep. 2001 1:1067. [PubMed: 11990500]

38. Cravatt BF, et al. Supersensitivity to anandamide and enhanced endogenous cannabinoid signaling in mice lacking fatty acid amide hydrolase. Proc Natl Acad Sci U S A. Jul 31.2001 98:9371. [PubMed: 11470906]

39. Liu W, et al. Role of neutrophil elastase in stress-induced gastric mucosal injury in rats. J Lab Clin Med. Nov.1998 132:432. [PubMed: 9823937]

40. Long JZ, Nomura DK, Cravatt BF. Characterization of monoacylglycerol lipase inhibition reveals differences in central and peripheral endocannabinoid metabolism. Chemistry & biology. Jul 31.2009 16:744. [PubMed: 19635411]

41. Leung D, Hardouin C, Boger DL, Cravatt BF. Discovering potent and selective reversible inhibitors of enzymes in complex proteomes. Nat Biotechnol. 2003; 21:687. [PubMed: 12740587]

42. Long JZ, et al. Dual blockade of FAAH and MAGL identifies behavioral processes regulated by endocannabinoid crosstalk in vivo. Proceedings of the National Academy of Sciences of the United States of America. Dec 1.2009 106:20270. [PubMed: 19918051]

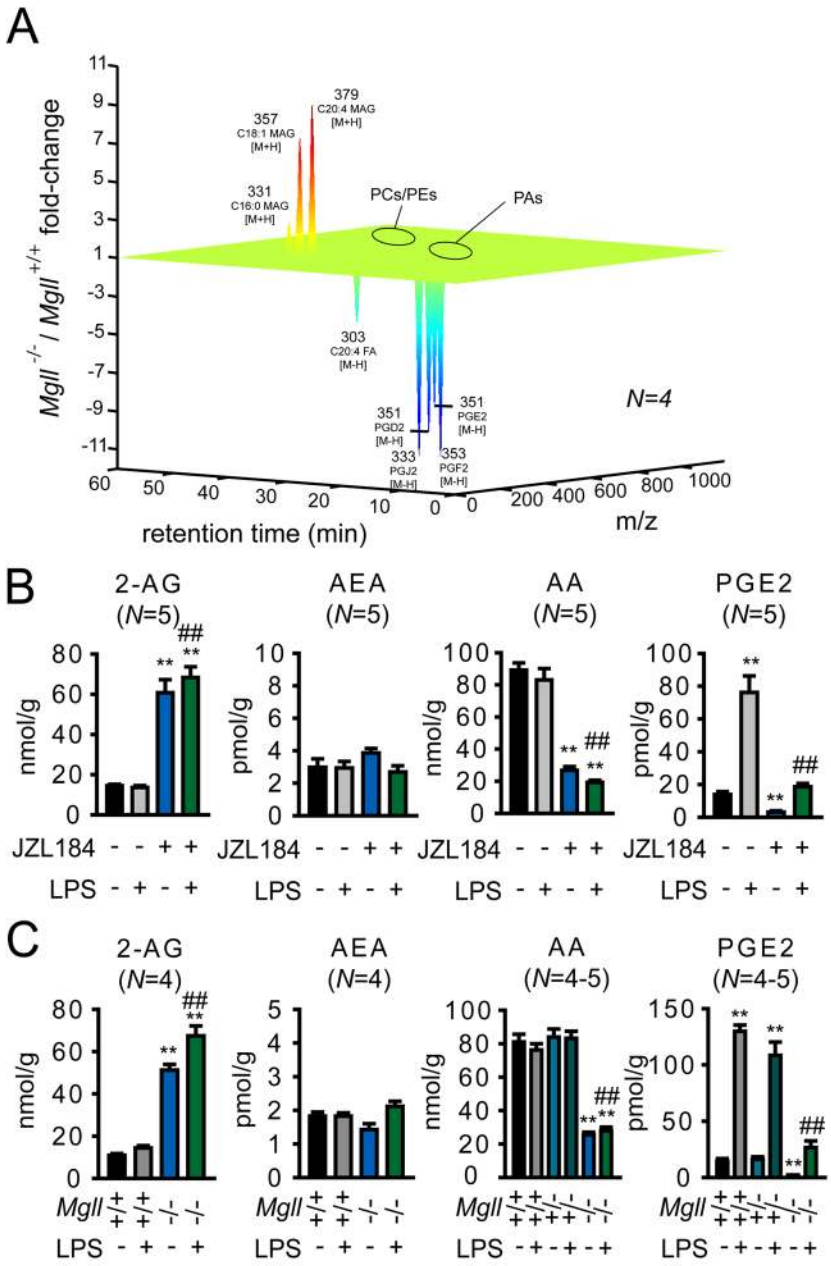

Fig. 1.

MAGL regulates an AA metabolic pathway in brain that includes both endocannabinoids and eicosanoids. **(A)** Metabolomic analysis of brain tissue from $Mgll^{+/+}$ and $Mgll^{-/-}$ mice. Organic extracts of $Mgll^{+/+}$ and $Mgll^{-/-}$ brains were analyzed by LC/MS in both the positive and negative ion mode by scanning a broad mass range between *m/z* 100–1200. Metabolite levels that showed a least a two-fold difference between $Mgll^{+/+}$ and $Mgll^{-/-}$ brains (with p values < 0.05) were determined by the software program XCMS (30) and these differences were confirmed by manual quantification of extracted ion peaks. Metabolites altered less than 2-fold are not included in the metabolomics plot. Abbreviations: phosphatidylcholine (PCs), phosphatidylethanolamines (PEs), and phosphatidic acids (PAs). Eicosanoids, which are too low in abundance for detection in brain tissue by untargeted mass scanning, were measured by targeted selected reaction monitoring. **(B)** Brain metabolite levels (determined

by selected reaction monitoring using LC/MS) from mice treated with the MAGL inhibitor JZL184 (40 mg/kg, ip) or vehicle 30 min prior to administration of LPS (20 mg/kg, ip, 6 h) or vehicle. **(C)** Brain metabolite levels from $Mgll^{+/+}$, $^{+/-}$, and $^{-/-}$ mice with or without LPS-treatment (20 mg/kg, ip, 6 h). *$p < 0.05$ and **$p < 0.01$ for LPS-treated, JZL184-treated, or $Mgll^{-/-}$ groups compared to vehicle or $Mgll^{+/+}$ group. ##$p < 0.01$ for JZL184/LPS-treated versus LPS-treated groups, or LPS-treated $Mgll^{-/-}$ versus LPS-treated $Mgll^{+/+}$ or $Mgll^{+/-}$ groups. No statistically significant differences were observed between $Mgll^{+/-}$ and $^{+/+}$ groups. Data shown are from mice sacrificed by rapid decapitation (see Supplemental Methods). Similar results were obtained with mice sacrificed by head-focused microwave irradiation, although the absolute brain levels of AA and PGs were 5–20-fold lower in these animals (Fig. S2) (17). Data are presented as average ± standard error of the mean (SEM). *N*=4–5 mice/group. Experiments were performed twice and one dataset is shown.

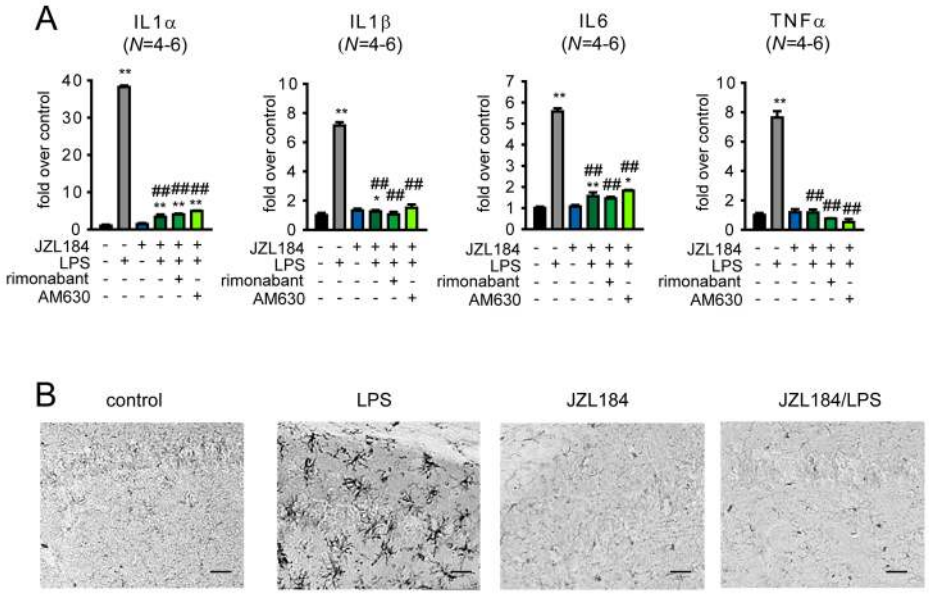

Fig. 2.

MAGL blockade impairs LPS-induced neuroinflammatory responses in the mouse brain. **(A)** Inflammatory cytokine levels as measured by quantitative ELISA in brain tissue from mice treated with JZL184 (40 mg/kg, ip) or vehicle administered 30 min prior to vehicle or LPS treatment (20 mg/kg ip, 6 h). The CB1 and CB2 antagonists rimonabant (1 mg/kg, ip) and AM630 (1 mg/kg, ip), respectively, were administered 30 min prior to JZL184 treatment. (B) Microglial activation assessed by Iba-1 staining (Iba-1 is marker of microglial cells and is upregulated upon activation of microglia) of hippocampal regions from LPS-treated (20 μg in 100 μl phosphate-buffered saline injected ip once per day for 4 d) or vehicle-treated mice administered vehicle or JZL184 (40 mg/kg, oral gavage, once per day for 4 d). Images were taken at 20x on a bright-field microscope. Panels in (B) are same magnification, scale bars 50 μm. $*p < 0.05$, $**p < 0.01$ for all groups compared to vehicle-treated control mice (A) . $\#\#p < 0.01$ for JZL184, rimonabant and/or AM630-treated/LPS-treated groups versus vehicle/LPS-treated groups. Data are presented as average ± SEM. N=4–6 mice/group. Experiments were performed twice and datasets were pooled for (A). A representative dataset is shown for (B).

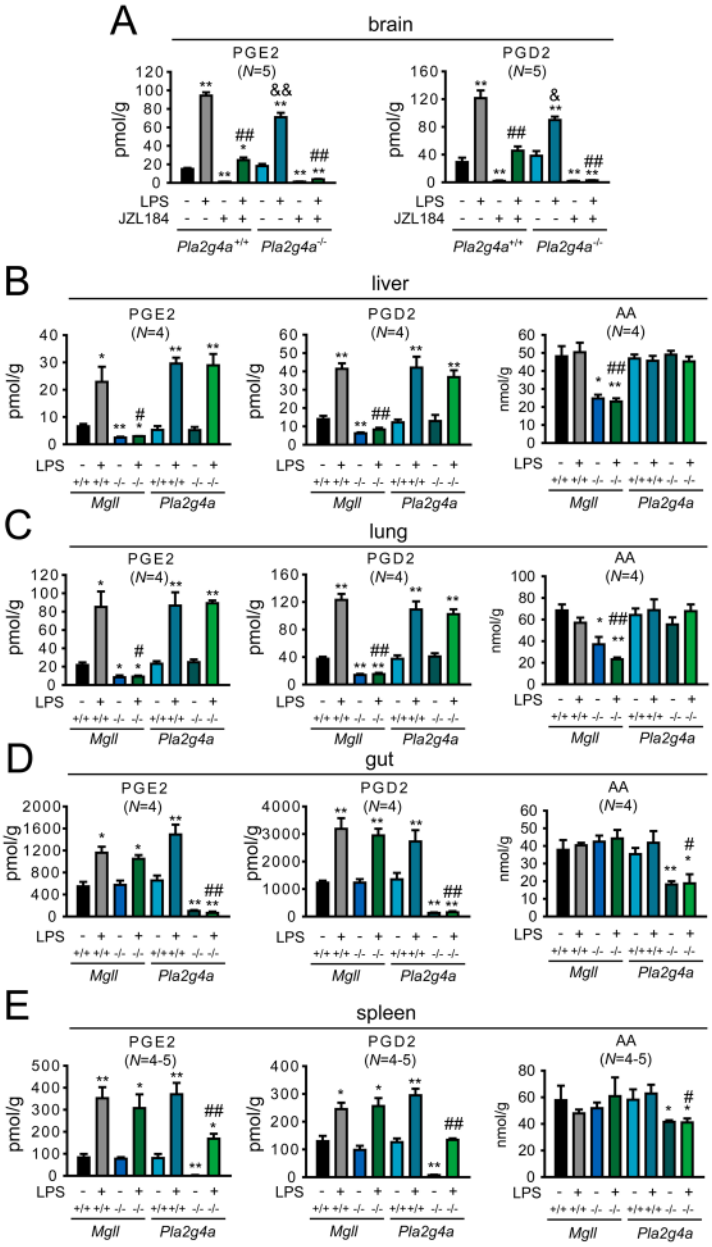

Fig. 3.

Anatomical portrait of the contributions that MAGL and cPLA2 make to eicosanoid metabolism in mice. **(A)** Brain metabolite levels determined by single ion monitoring by LC/MS from *Pla2g4a*$^{+/+}$ and $^{-/-}$ mice treated with JZL184 (40 mg/kg, ip) or vehicle 30 min prior to administration of LPS (20 mg/kg ip, 6 h) or vehicle. **(B to E),** Metabolite levels in liver **(B)**, lung **(C)**, gut **(D)** and spleen **(E)** tissue from *Mgll*$^{+/+}$, *Mgll*$^{-/-}$, *Pla2g4a*$^{+/+}$, and *Pla2g4a*$^{-/-}$ mice following administration of LPS (20 mg/kg ip, 6 h) or vehicle. $^{**}p < 0.01$ for all groups compared to the vehicle-treated *Pla2g4a*$^{+/+}$ group in **(A)**, and *Mgll*$^{-/-}$ versus *Mgll*$^{+/+}$ groups or *Pla2g4a*$^{-/-}$ versus *Pla2g4a*$^{+/+}$ groups for **(B).** $\#\#p < 0.01$ for *Pla2g4a*$^{+/+}$ or *Pla2g4a*$^{-/-}$ groups treated with JZL184/LPS versus the *Pla2g4a*$^{+/+}$ group treated with vehicle/LPS. $\&\&p < 0.01$ for *Pla2g4a*$^{-/-}$mice treated with LPS versus *Pla2g4a*$^{+/+}$ mice

treated with LPS. Data are presented as average ± standard error mean (SEM); n = 4–5 mice/group. Experiments were performed twice and one representative dataset is shown.

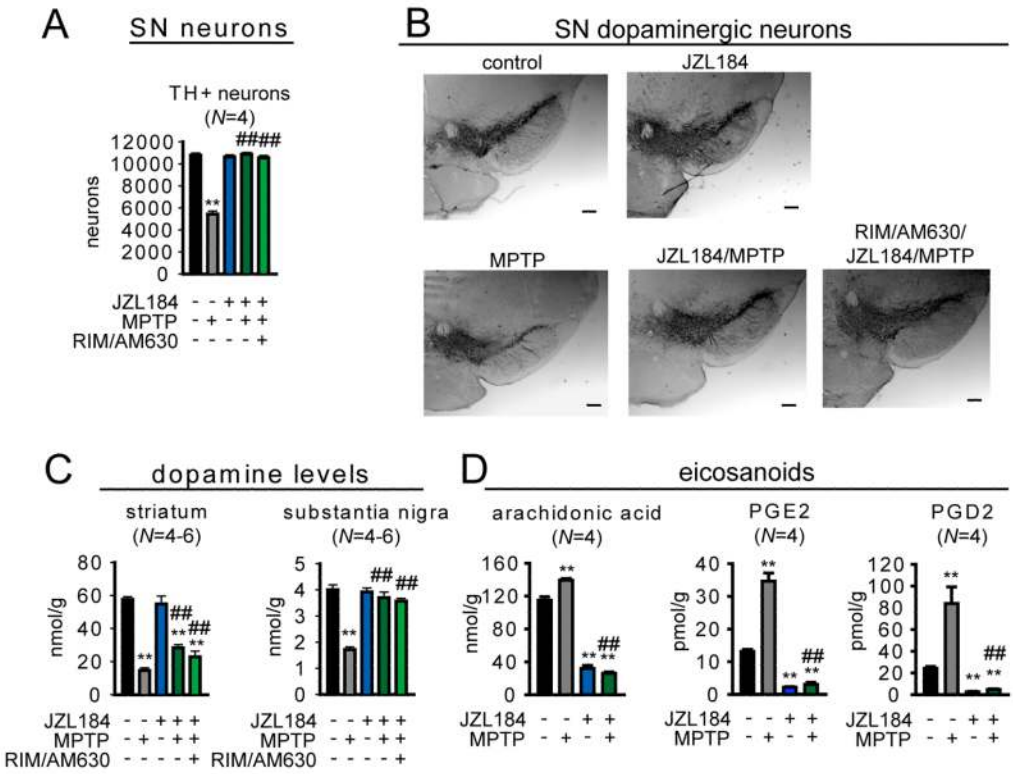

Fig. 4.

MAGL blockade protects against MPTP-induced dopaminergic neurodegeneration. (**A**) Number of dopaminergic neurons as measured by counting tyrosine hydroxylase (TH)-positive cells in the substantia nigra of JZL184-treated (40 mg/kg oral gavage; daily treatment starting 1 day prior to MPTP administration) versus vehicle-treated mouse groups. AM630/rimonabant (formulated together, 10 mg/kg, oral gavage) was administered 30 min prior to JZL184 treatments. (**B**) Representative images of the substantia nigra of JZL184-, AM630/rimonabant/JZL184- versus vehicle-treated mouse groups. Neurons were detected by tyrosine hydroxylase staining of fixed sections of the substantia nigra. Images were taken at 4 x with a brightfield microscope. Panels in (B) are same magnification, scale bars 200 μm. (**C**) Dopamine levels as measured by LC/MS in the striatum and substantia nigra of JZL184- versus vehicle-treated mouse groups. (**D**) Whole-brain eicosanoid levels from JZL184- versus vehicle-treated mouse groups. MPTP treatment consisted of 4 doses of 15 mg/kg ip every 2 hours. Eicosanoid levels were measured 1 day after initial MPTP treatments. Dopaminergic neuron count and images and dopamine levels were obtained 7 days after initial MPTP treatments. $^{**}p < 0.01$ for all groups compared to vehicle-treated control mice. $^{\#\#}p < 0.01$ for all JZL184-treated MPTP groups versus vehicle-treated MPTP groups. Data are presented as average ± SEM; $N = 4–6$ mice/group. Experiments were performed twice and one representative dataset is shown.